



## Microalgal biochemical composition dynamics and gene expression in response to bacterial quorum sensing signals

Shahla Radmehr<sup>a,b,\*</sup>, Johanna M. Rinta-Kanto<sup>b</sup>, Ville Santala<sup>b</sup>, Mika Mänttari<sup>a</sup>

<sup>a</sup> Department of Separation Science, LUT School of Engineering Science, Lappeenranta-Lahti University of Technology LUT, Yliopistonkatu 34, 53850, Lappeenranta, Finland

<sup>b</sup> Faculty of Engineering and Natural Sciences, Tampere University, Hervanta Campus, 33720, Tampere, Finland

### ARTICLE INFO

#### Keywords:

Quorum sensing  
Cellular communication  
Microalgae  
Bacteria  
Lipid  
polysaccharide

### ABSTRACT

Microalgae are promising resources for biofuels and bioproducts due to their ability to accumulate high-value metabolites such as lipids and polysaccharides. To enhance the production of these target bioproducts, an emerging strategy is to harness bacterial quorum sensing signals (QSSs) as cross-kingdom cues to steer algal metabolism, rather than relying solely on stress regimes or genetic modification, which can slow growth or cause regulatory limitations. N-acyl homoserine lactones (AHLs), particularly those present in activated sludge, are natural signaling molecules that may reprogram microalgal metabolism. However, the transcriptomic effects and species-specific responses to these signals remain poorly understood. In this study, three model microalgal strains—*Chlamydomonas reinhardtii*, *Chlorella vulgaris*, and *Scenedesmus quadricauda*—were exposed to pure N-hexanoyl-L-homoserine lactone (C6-HSL) and activated sludge-derived AHLs (AS-AHLs) to evaluate their potential for metabolic steering. Transcriptomic and phenotypic analyses revealed species-specific metabolic responses to AHLs. Fatty acid synthesis genes were upregulated mainly in *Chlorella* and *Scenedesmus*, supporting increased lipid accumulation, while *Chlamydomonas* redirected part of carbon flux toward polysaccharide biosynthesis. Lipid content increased by up to 26%, and polysaccharides by 45% in *Chlamydomonas*. *Scenedesmus* showed the highest lipid accumulation increase, reaching 33%. Meanwhile, C6-HSL treatment led to significant changes in gene expression, particularly suppression of TCA cycle and DNA replication genes in *Chlamydomonas* and *Chlorella*, consistent with a shift toward energy conservation. In contrast, *Scenedesmus* showed minimal transcriptional changes, suggesting greater metabolic stability. Additionally, AHLs promoted microalgal aggregation, potentially aiding biomass harvesting. These findings highlight potentials of leveraging microbial signals to manipulate algal metabolic outputs.

### 1. Introduction

Microalgae biomasses have significant promise for diverse applications, including the production of bioplastics, feed/food supplements, and biofuels (Rajpoot et al., 2022; Udayan et al., 2021). The utility of different microalgae cells is linked to the composition of their biomass, specifically in proteins, lipids, polysaccharides, and pigments (Wu et al., 2021). These compositions vary depending on the microalgal strain and cultivation conditions. Some selected microalgae strains such as *Scenedesmus*, *Chlamydomonas*, *Chlorella*, and *Dunaliella* can accumulate polysaccharides over 20% of their dry weight (Gouda et al., 2022). Microalgal polysaccharides have attracted attention in recent years due to their wide range of applications in food, cosmetics, and health sectors

(Caetano et al., 2022). The lipid content of microalgae is also notable, with some species outperforming traditional oil crops like soybean, sunflower, and corn (Udayan et al., 2023). Microalgae such as *Chlorella* and *Chlamydomonas* are famous for producing lipid content ranging from 10% to 30% of their dry weight (Deshmukh et al., 2019; Ferreira et al., 2019). Microalgal lipids predominantly include triacylglycerols, which are non-polar lipids formed by esterifying three fatty acids with glycerol. Microalgae cells exhibit a diverse range of fatty acids, including short-chain, medium-chain, and long-chain fatty acids. Additionally, polyunsaturated fatty acids (PUFAs) like docosapentaenoic acid and eicosapentaenoic acid have been identified, and play key roles in the food industry (Mangope et al., 2025).

Microalgae are considered promising feedstocks for lipid production,

\* Corresponding author at: Faculty of Engineering and Natural Sciences, Tampere University, Hervanta Campus, 33720, Tampere, Finland.

E-mail address: [Shahla.radmehr@tuni.fi](mailto:Shahla.radmehr@tuni.fi) (S. Radmehr).

<https://doi.org/10.1016/j.biteb.2026.102778>

Received 23 October 2025; Received in revised form 9 April 2026; Accepted 25 April 2026

Available online 27 April 2026

2589-014X/© 2026 The Authors. Published by Elsevier Ltd. This is an open access article under the CC BY license (<http://creativecommons.org/licenses/by/4.0/>).

but their large-scale application remains limited by low productivity and the difficulty of increasing lipid accumulation (Sreelakshmi and Arunkumar, 2025). To increase the yield of specific biomolecules including lipid and polysaccharide in microalgae biomass, different approaches have been investigated, such as pH modification, carbon source alterations, metabolic engineering, and variations in light intensity and photoperiods (Behera et al., 2021). Adams et al. (2013) showed that subjecting microalgae to stress conditions, such as limiting nutrient availability—particularly nitrogen—can enhance the production of valuable biomolecules like lipids in microalgal biomass. However, further studies are needed to identify more efficient strategies for optimizing biomolecule production in diverse microalgal species.

Quorum sensing signals (QSSs) are small molecules that mediate bacterial cell-to-cell communication (Mukherjee and Bassler, 2019). N-acyl homoserine lactones (AHLs), which are also present in activated sludge, are well-characterized QSSs in Gram-negative bacteria and are increasingly recognized as key interkingdom cues that can reprogram microalgal metabolism and stimulate lipid production (Coolahan and Whalen, 2025; Zhang et al., 2018). Additionally, recent reviews have summarized how QSSs can alter microalgal growth and metabolism, acting as direct effectors of photosynthesis, regulators of the cell cycle, and modulators of algicidal or growth-promoting interactions (Dow, 2021). Metagenomic and reactor-scale studies further indicate that QSSs are enriched in algal systems and can strongly shape algal–bacterial consortia and reactor performance in wastewater treatment (Wu et al., 2022). Beyond this ecological role, several experimental studies have shown that exogenous AHLs or sludge-derived QS extracts can enhance nutrient removal in algal–bacterial consortia (Lyu et al., 2022). These studies support the view that QSSs, including AHLs present in activated sludge, can act as natural cross-kingdom metabolic triggers that influence microalgal growth and storage metabolism.

However, despite this progress, several key gaps remain. Most studies have treated QSSs mainly as stress factors and have focused on bulk responses such as growth, total lipid content, nutrient removal, and flocculation, with limited insight into how these natural metabolic triggers reorganize central metabolism and storage pathways in algae. Moreover, there is a lack of comparative, species-resolved transcriptomic data describing how different microalgae respond to AHLs, and how these transcriptional programs influence carbon partitioning into lipid and polysaccharide storage remains unclear. Additionally, because QSSs can affect different pathways like photosynthesis, carbon partitioning, stress responses, and cell-cycle control, transcriptomic analysis is necessary to capture the system-wide reprogramming they induce, to identify the metabolic pathways and regulatory modules that are differentially engaged in each species. Here, we conceptualize QSSs as a molecular language used by bacteria to reprogram algal metabolism. The novelty of this study lies in integrating metabolic and transcriptomic analyses across different microalgal species to determine how these signals drive species-specific lipid and polysaccharide accumulation, as well as aggregation behaviors, beyond what can be inferred from bulk chemical analyses alone.

In this study, three widely cultivated microalgal strains — *Chlorella vulgaris*, *Chlamydomonas reinhardtii*, and *Scenedesmus quadricauda* — were exposed to pure C6-HSL and naturally derived AHLs extracted from activated sludge. The hypothesis is that AHL exposure induces species-specific transcriptomic reprogramming that redirects central carbon metabolism toward distinct storage outcomes (lipid versus polysaccharide accumulation). By analyzing detailed changes in polysaccharide, lipid, and fatty acid profiles, we reveal how QSSs can act as cross-kingdom stress-related signals that reprogram metabolite production and aggregation behavior in a species-specific manner. Importantly, integrated mRNA expression analysis demonstrates, at the genomic level, how AHL exposure fundamentally rewires key metabolic pathways, thereby enhancing the synthesis of valuable compounds without any genetic modification. The environmentally relevant use of AS-AHLs directly mimics natural chemical signals present in

wastewater, offering a practical, low-input strategy for sustainably increasing high-value metabolite yields while improving harvesting efficiency in large-scale algal bioprocesses.

## 2. Materials and methods

### 2.1. Microalgae cultivation and growth measurement

The microalgae cells (*Chlorella vulgaris*, *Chlamydomonas reinhardtii*, and *Scenedesmus quadricauda*) were cultivated in TAP (Tris–acetate–phosphate) media at pH 7 and 23–24 °C for 6 days, and then the biomass underwent centrifugation at 5000 rpm for 5 min. These microalgae cells were selected because they are model species for biofuel and bioproduct research, represent different phylogenetic lineages and cell morphologies, and are commonly used in wastewater and algal–bacterial systems, making them highly relevant for both fundamental and applied studies (Mohamed et al., 2025; Scranton et al., 2015; Sun et al., 2025). Subsequently, the harvested biomass was washed and re-suspended in autoclaved TAP media. Cell growth was assessed by measuring the optical density at 750 nm (OD750) using UV/VIS spectrophotometry. Specific growth rate ( $\mu$ ) and biomass productivity (P) of *Chlamydomonas reinhardtii*, *Chlorella vulgaris*, and *Scenedesmus quadricauda* under control, C6-HSL, and AS-AHL treatments over 6 days, calculated from biomass at day 0 and day 6 using  $\mu = \ln(X_6/X_0)/(t_6 - t_0)$  and  $P = (X_6 - X_0)/(t_6 - t_0)$ .

### 2.2. Experimental protocol

Activated sludge was sourced from the aeration tank of a wastewater treatment plant located in Lappeenranta, Finland. N-Acyl homoserine lactones were extracted as described in Wang et al. study (Wang et al., 2017). Briefly, 500 mL activated sludge centrifugation at 5000 rpm for 15 min. The resulting supernatant was then mixed with an equal volume of acidified ethyl acetate (0.1% acetic acid) and sonicated at 4 °C for 20 min. This mixture underwent thorough mixing for 24 h and was subsequently allowed to settle for 15 min. The upper layer was collected and dried using liquid nitrogen. The extracted samples were analyzed by high performance liquid chromatography (HPLC agilent) with DAD detector at 210 nm. The used column was Phenomenex Kinetex 2.6  $\mu$ m, C18 100 Å (150 × 3 mm). Linear gradient elution (MeOH+0.1% Acetic acid) with flow rate of 0.2 mL minute<sup>-1</sup> was used. To further test the effects of pure QSSs on microalgae strains, C6-HSL (N-hexanoyl-L-Homoserine lactone, Sigma) was utilized. Based on HPLC quantification, the AS-AHL extract was standardized and diluted to a final working concentration equivalent to 5  $\mu$ M C6-HSL in the algal cultures. C6-HSL was specifically selected for this study because it is a dominant AHL in activated sludge and wastewater systems (Wang et al., 2022), highlighting its potential for cost-effective production. Additionally, its medium chain length provides a good balance between membrane permeability and solubility, making it experimentally robust, and previous studies have shown that C6-HSL can enhance nutrient removal and promote lipid production in microalgae (Lyu et al., 2022), supporting its choice in this study. The samples are supplemented with 5  $\mu$ M C6-HSL. This dose was selected based on previous study reporting measurable microalgal responses within this concentration range (Zhang et al., 2018). The pure flask of *Chlamydomonas*, without any QSSs, was labeled as Chlmy-P. Flask with pure C6-HSL were named Chlmy-C6, while the one with AHLs extracted from activated sludge was named Chlmy-AS. The same pattern was used to name *Chlorella* (Chl–P, Chl–C6, and Chl–AS) and *Scenedesmus* (Sc–P, Sc–C6, and Sc–AS). All experimental protocols were carried out in triplicate.

### 2.3. Analysis of microbial attachment

To assess the impact of QSSs on attachment potential of microalgae, 20 mL of biomasses from all flasks were transferred into Petri dishes. The

Petri dishes underwent 24 h incubation at 30 °C. After incubation the biomass was removed from the Petri dishes and washed with distilled water three times and then dried at 60 °C for 30 min. Subsequently, 0.1% (w/v) crystal violet solution was added to each Petri dish and left for 15 min. The Petri dishes were then rinsed with distilled water. The microscopic observations of the attached microorganisms were conducted using an Olympus microscope.

#### 2.4. Polysaccharide and lipid determination

Approximately 2–3 mg of dry biomass was weighed, and 4 mL of 0.9% NaCl solution was added for homogenization. The sample was incubated at 100 °C for 15 min, followed by centrifugation. The supernatant was collected, and the sulfuric acid-phenol method was used for polysaccharide quantification (DuBois et al., 1956). A modified Bligh and Dyer method was employed for total lipid extraction. Approximately 2 mg of dry microalgae biomass was suspended in a 10 mL mixture of chloroform and methanol (1:2 ratio) and sonicated for 30 min on ice (Iverson et al., 2001). Subsequently, 3.4 mL of chloroform and 3 mL of water were added to the tubes, followed by an additional 10 min of sonication. The resulting bottom layer was extracted, and a known volume was transferred into pre-weighed trays. The samples were subjected to evaporation and subsequent drying. The dried lipids were then weighed to determine the recoverable lipid content. The fatty acids were extracted with chloroform–methanol (2:1 v/v) and methanol-sulfuric acid (1%) and were analyzed with Shimadzu QP2010-Ultra GC–MS.

#### 2.5. Observation of intercellular chlorophyll and lipid with confocal microscopy

To visualize chlorophyll and lipid components within microalgae cells, both with and without AHLs, confocal laser scanning microscopy (Zeiss LSM 710) was employed. Chlorophyll was observed at a 40× magnification based on its autofluorescence. The excitation of chlorophyll was achieved using a 633-nm laser, and observations were made in the channels ranging from 647 to 743 nm (emission). For lipid observation, samples were stained with Nile red ( $\epsilon$ : 38000 cm<sup>-1</sup> M<sup>-1</sup>). Specifically, 100  $\mu$ L of samples were mixed with 100  $\mu$ L of 1  $\mu$ g mL<sup>-1</sup> Nile Red in a 1:1 (vol/vol) DMSO: water solution. The plate was then incubated for 15 min at 37 °C. Nile red dye was excited using the 533-nm line laser, and observations were made in the channel at 530–570 nm.

#### 2.6. RNA extraction, sequencing, and bioinformatics

After extracting RNA from pure microalgae cells and the one which were treated with C6-HSL using Zymo kits, the samples were sent to Novogene for sequencing on dry ice. Novogene purified mRNA using poly-T magnetic beads, fragmented it, and synthesized cDNA using random hexamer primers. Directional (dUTP) or non-directional (dTTP) libraries were prepared and quantified with Qubit and real-time PCR. Libraries were pooled and sequenced on an Illumina platform, generating paired-end reads. The raw sequencing data in FASTQ format was processed to remove adapters, poly-N sequences, and low-quality reads, generating clean data for downstream analysis. Trinity was used for transcriptome assembly, followed by redundancy removal with CORSET. Finally, BUSCO was used to provide a quantitative assessment of the completeness in terms of expected gene content of transcriptome. Gene expression levels were quantified using RSEM. Differential expression analysis was conducted using DESeq2 (with replicates). Data with an adjusted *P* value <0.05 were assigned as differentially expressed.

### 3. Results

#### 3.1. Growth rate and attachment of microalgae

Fig. S1 (Supporting Information: growth profile) shows the impact of pure C6-HSL and activated sludge-extracted AHLs (AS-AHLs) on the growth rates of three microalgae species, *Chlamydomonas*, *Chlorella*, and *Scenedesmus*. Fig. S1a shows that Chlamy-P and Chlamy-C6 had similar growth rates ( $P > 0.05$ , *t*-test). However, exposure to AS-AHLs signals delayed the stationary phase and significantly ( $P < 0.05$ , *t*-test) inhibited the optical density by 20% compared to Chlmay-P at day 6. All *Chlorella* flasks (Fig. S1b), regardless of AHLs presence, reached the stationary phase at day 4. However, presence of both C6-HSL and AS-AHLs in cultivation flasks exhibited a significant reduction ( $P < 0.05$ , *t*-test) in *Chlorella* growth rate, with AS-AHLs inducing more effects on *Chlorella*. Additionally, growth results highlight the distinct growth trend of *Scenedesmus* compared to the other microalgae. In contrast to the effects observed in *Chlamydomonas* and *Chlorella*, neither C6-HSL nor AS-AHLs had a significant effect ( $P > 0.05$ , *t*-test) on the growth rate of *Scenedesmus* (Fig. S1c). Consistently, Table S1 summarizes the specific growth rates ( $\mu$ ) and biomass productivities (*P*) over 6 days, confirming that both C6-HSL and AS-AHLs decreased  $\mu$  and *P* in *Chlamydomonas* and *Chlorella*, while the values for *Scenedesmus* remained largely unchanged compared with the other two species. Aggregation results (Supporting Information (Fig. S2): Microalgae attachment) show the crystal violet-stained microalgal attachment on petri dish surfaces. The findings clearly reveal increased microbial attachment in the presence of both C6 and AS-AHLs across all three microalgal strains. Notably, the images for *Scenedesmus* clearly demonstrate a greater microbial attachment in the presence of AS-AHLs compared to C6-HSL. Apart from the increased aggregation observed under AHL treatments (shown in Fig. S2), no other clear morphological changes were detected in the three algal strains.

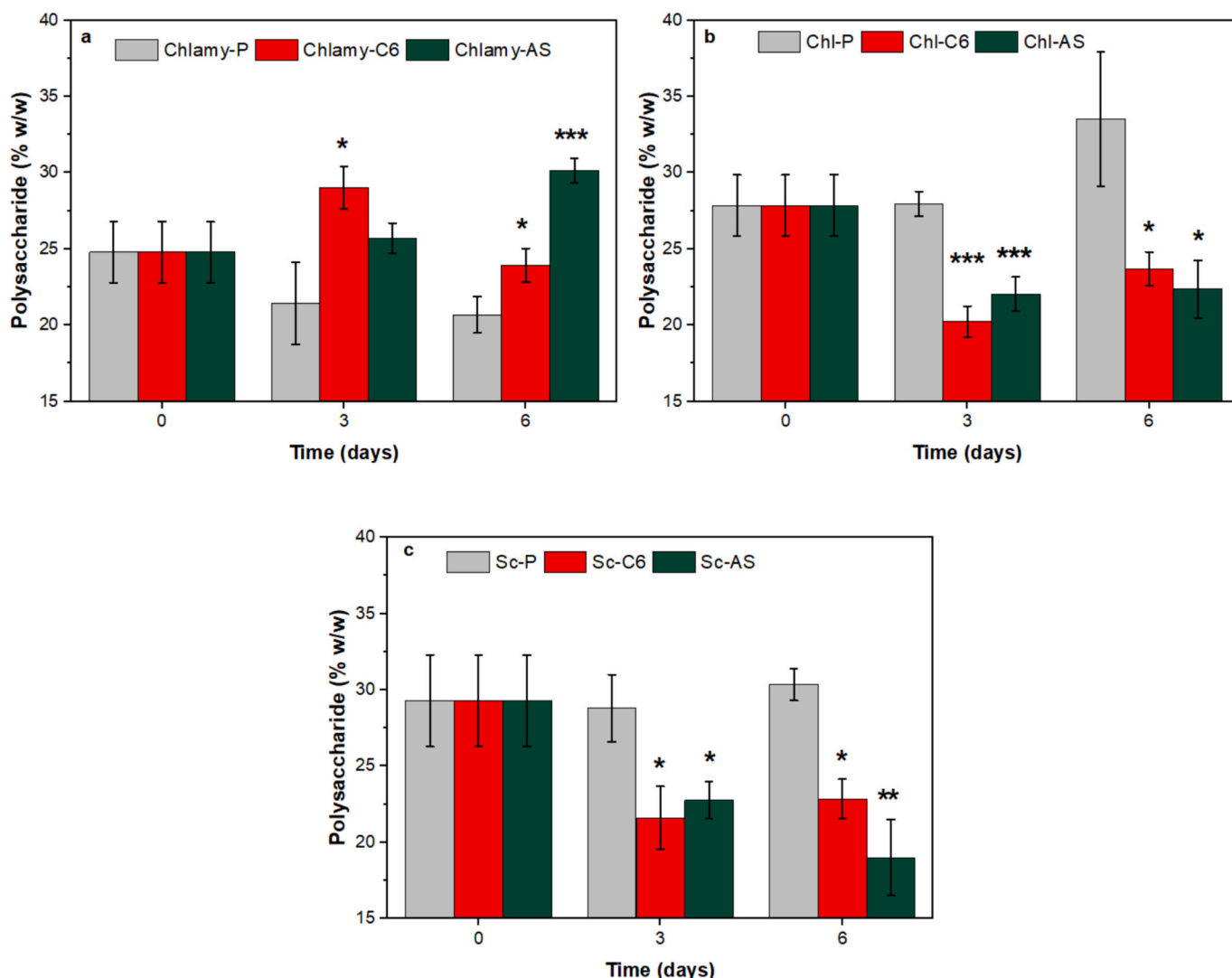
#### 3.2. Polysaccharide under QSSs treatment

Fig. 1 shows the polysaccharide content in microalgae cultures under varying AHL conditions. In *Chlamydomonas* (Fig. 1a), the presence of AHLs resulted in an increase in polysaccharide accumulation. While the polysaccharide content slightly reduced after 6 days for Chlamy-P without any AHL treatment. At day 6, compared with Chlamy-P, there was an approximately 45% and 15% increase in polysaccharide amount in Chlamy-AS and Chlamy-C6, respectively. Turning to *Chlorella* (Fig. 1b), both Chl-C6 and Chl-AS had close polysaccharide content, which was approximately 30% less than Chl-P at day 6. The effect of AHLs on *Scenedesmus* was similar to *Chlorella*, resulting in a reduction in polysaccharide accumulation.

#### 3.3. Lipid accumulation under QSSs treatment

In *Chlamydomonas*, lipid accumulation increased by around 20% and 17% with the addition of pure C6-HSL and AS-AHLs at day 3 compared to pure culture (Fig. 2) and at day 6 around 26% more lipid found in pure C6-HSL compared with pure culture. In *Chlorella* at day 3, C6-HSL treatment resulted in 16% lower lipid accumulation, whereas AS-AHLs slightly promoted higher lipid accumulation to the pure culture. However, at day 6, C6-HSL enhanced lipid accumulation. In *Scenedesmus*, lipid accumulation consistently increased with both C6-HSL and AS-AHL treatments, compared to the pure culture. At day 3, Sc-AS shows around 33% more lipid compared to Sc—P. These findings highlight the species-specific effects of AHL treatments, with *Scenedesmus* showing the most pronounced lipid accumulation under AS-AHL conditions.

The fatty acid profiles of microalgae cells under different QSSs treatments at day 6 are detailed in Table S2 (Supporting Information: fatty acid profile). Table S2 shows that in *Chlamydomonas*, treatment with AS-AHL led to a notable increase of saturated fatty acids (C16:0 increased to 34.4%) compared to pure culture (23.7%), while the



**Fig. 1.** Polysaccharide profiles of microalgae cells: a) *Chlamydomonas* (Chlamy.), b) *Chlorella* (Chl.), and c) *Scenedesmus* (Sc.) with/without quorum sensing signals. Data represent the mean values of triplicates and error bars show the standard deviation. Asterisk indicates significant difference between control and treatments according to one-way ANOVA (Tukey's test) (\* $P < 0.05$ , \*\* $P < 0.01$ , \*\*\* $P < 0.001$ ).

percentage of mono-unsaturated fatty acids (MUFAs), such as C18:1n9t, decreased, indicating a shift toward more saturated lipid profiles under AS-AHLs influence. For *Chlorella*, the addition of QSSs decreased the proportion of saturated fatty acids and poly-unsaturated fatty acids (PUFAs), while MUFAs, such as C18:1, increased in response to AHLs treatment (Table S2). In *Scenedesmus*, both C6-HSL and AS-AHL treatments led to minor changes in saturated fatty acids but caused significant alterations in unsaturated fatty acid profiles. AS-AHLs increased the proportion of MUFAs, particularly C16:1 (14.2%) compared to the pure culture (3.7%), while PUFAs, such as C18:3 N3, decreased under quorum sensing conditions (Table S2). These results reveal that QSSs induce distinct shifts in fatty acid composition across microalgae species while generally promoting higher MUFA content and reducing PUFA levels except for *Chlamy-AS*.

The Confocal laser scanning microscopy (CLSM) images (Fig. 3) which were gathered at day 4 reveal the presence of chlorophyll and triacylglycerol (TAG) inside microalgae cells, both with and without QSSs. In pure microalgae cultures, certain individual cells contain a minor quantity of TAG. Upon the introduction of QSSs to microalgae cultures, the received signal for TAG (yellow- partially shown by white dash circles) increased from the cells, while there is a reduction in chlorophyll signals (red) in the same cells. This increase in TAG signals,

which is in agreement with Fig. 2, validates that the presence of QSSs could direct the cells toward storage compounds when growth is hindered by QSSs.

### 3.4. RNA sequencing results

Fig. 4 presents gene ontology (GO) analysis for all three microalgae treated with C6-HSL compared with control samples to determine how C6-HSL, as a cross-kingdom signal, influences gene expression in algae and how these changes may correspond to the observed experimental data.

Fig. 4a shows GO enrichment bar chart of *Chlamydomonas* treated with C6-HSL compared with control sample. Notably, some genes involved in carbohydrate metabolism in *Chlamydomonas* showed increased expression in response to C6-HSL (Fig. 4a). These genes, including glucosamine-6-phosphate isomerase ( $-\log(\text{padj}) = 4.7$ ), phosphoglucomutase ( $-\log(\text{padj}) = 2.9$ ), and 1,3-beta-glucan synthase ( $-\log(\text{padj}) = 6.3$ ), are linked to glycolysis and glycosylation pathways. They generate key intermediates like glucose-6-phosphate, which facilitate the synthesis of polysaccharides. Additionally, the results show higher expression of polysaccharide deacetylase which suggests enhanced cell wall modification, contributing to cellular protection. The

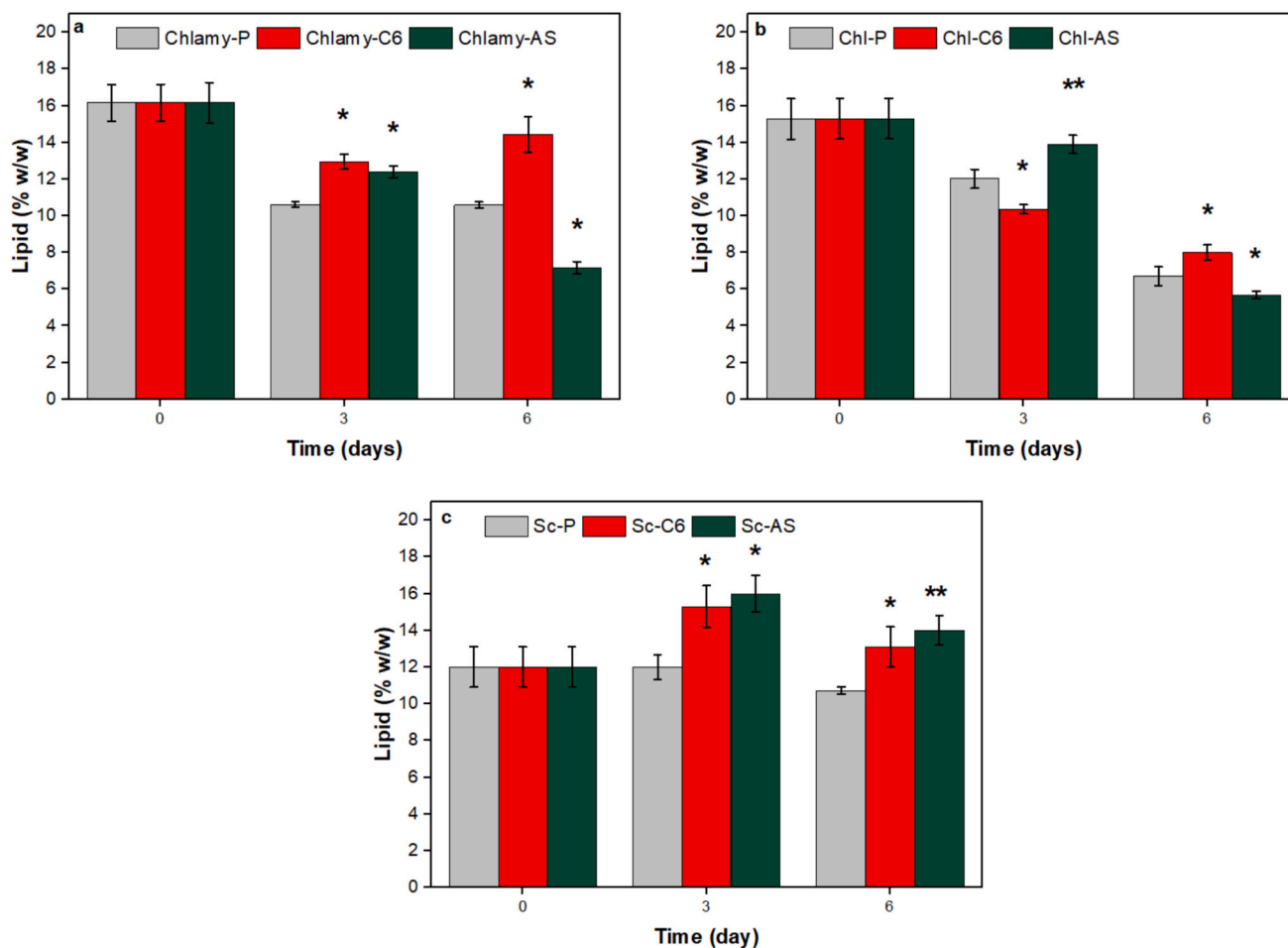


**Fig. 2.** Lipid profiles of microalgae cells: a) *Chlamydomonas* (Chlamy.), b) *Chlorella* (Chl.), and c) *Scenedesmus* (Sc.) with/without quorum sensing signals. Data represent the mean values of triplicates and error bars show the standard deviation. Asterisk indicates significant difference between control and treatments according to one-way ANOVA (Tukey's test) (\* $P < 0.05$ , \*\* $P < 0.01$ , \*\*\* $P < 0.001$ ).

enhanced carbohydrate metabolic flux through these pathways, induced by C6-HSL, likely contributed to the accumulation of polysaccharides in the treated sample, consistent with the results from Section 3.2.

Fig. 4a shows that overall ribosome biogenesis showed higher expression in response to C6-HSL treatment. However, genes related to 40S and 60S ribosomal proteins exhibited both up- and down-regulation, indicating finely tuned translational reprogramming rather than a uniform change. Higher expressed genes include stress-related proteins such as HSP70 chaperones (e.g., GRP78/BiP and GRP75/mortalin;  $-\log(\text{padj}) = 3.9$ ), which support protein folding and are known to be cold-inducible (Maikova et al., 2016). Also elevated is cysteine desulfurase ( $-\log(\text{padj}) = 17.3$ ), linked to mitochondrial function and oxidative stress resistance (Braymer and Lill, 2017). In contrast, several ribosome-related genes are showed lower expression, including fibrillarlin ( $-\log(\text{padj}) = 23.6$ ), uL4m ( $-\log(\text{padj}) = 22.2$ ), and rRNA methyltransferases ( $-\log(\text{padj}) = 18.5$ ), all of which are vital for rRNA modification and nucleolar ribosome assembly (Pereira-Santana et al., 2020). Genes associated with antioxidant activity also showed higher expression.

Fig. 4b shows effects of C6-HSL on gene expression profile of *Chlorella*. The genes with higher expressions included those related to catalytic and hydrolase activities can enhance enzymatic processes maybe linked to protein turnover and modification. There was also an increased expression of vesicle-mediated transport genes in *Chlorella*. This includes vesicle coat proteins like Clathrin heavy chain ( $-\log(\text{padj}) = 5.1$ ), COPI ( $-\log(\text{padj}) = 10.2$ ), and COPII ( $-\log(\text{padj}) = 8.9$ ), which form vesicles for cargo transport (Bykov et al., 2017). However, lower

expressions (Fig. 4b) observed in pathways are crucial for metabolic and structural integrity, such as ribosome structure and biogenesis, and photosynthesis-related genes, particularly those connected to the thylakoid. Moreover, the addition of C6-HSL to *Chlorella* resulted in lower expression of genes involved in the carbohydrate metabolic process, aligning with the observed reduction in carbohydrate content in the biomass (Fig. 1). Key enzymes such as fructose-bisphosphate aldolase ( $-\log(\text{padj}) = 33.7$ ), 3-phosphoglycerate kinase ( $-\log(\text{padj}) = 31$ ), and glycogen phosphorylase ( $-\log(\text{padj}) = 28.3$ ) showed lower expression.

In *Scenedesmus* algae treated with C6-HSL, gene expression analysis (Fig. 4c) shows that there is a higher expression in genes related to transporter activity and transmembrane transport. However, key carbohydrate metabolism genes showed lower expression after C6-HSL treatment, similar to patterns seen in *Chlorella* (Fig. 1). Genes like fructose-bisphosphate aldolase ( $-\log(\text{padj}) = 9.5$ ), mannose-6-phosphate isomerase ( $-\log(\text{padj}) = 21.2$ ), and carbonic anhydrase ( $-\log(\text{padj}) = 32.9$ ) showed reduced expression.

### 3.5. Regulation of TCA cycle and fatty acid biosynthesis genes

Fig. 5a illustrates the main genes involved in the TCA cycle and important pathways for fatty acid biosynthesis. Transcriptomic analysis (Supporting Information Table S3a: differential gene expression in TCA cycle) highlights that C6-HSL treatment mainly downregulates the TCA cycle genes in *Chlamydomonas*, with notable suppression of key enzymes. Table S3a shows that succinate dehydrogenase and isocitrate

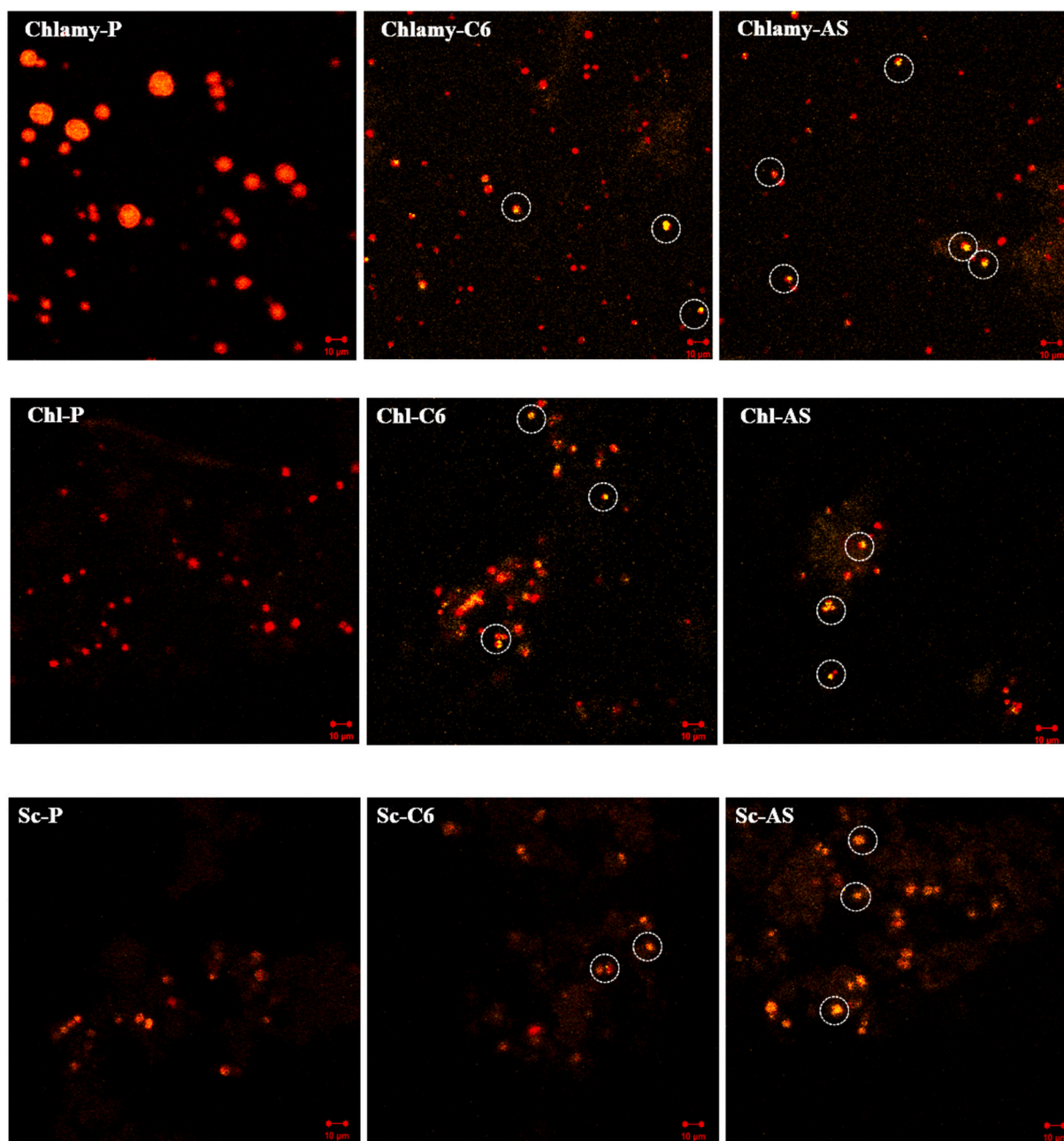


**Fig. 3.** Confocal laser scanning microscopy of different microalgae cultures (*Chlamydomonas* (Chl.), *Chlorella* (Chl.), and *Scenedesmus* (Sc.)) with and without quorum sensing signals. The autofluorescence chlorophyll and stained TAG were detected in red and yellow, respectively. (For interpretation of the references to colour in this figure legend, the reader is referred to the web version of this article.)

dehydrogenase have consistent lower expression which indicates a significant reduction in electron transport and TCA cycle flux. Citrate synthase, a critical entry point enzyme, also shows strongly lower expression. In contrast, malate dehydrogenase shows a mixed response, with two genes expressed higher and one expressed lower. For *Chlorella* results show lower expression of key enzymes like malate dehydrogenase and 2-oxoglutarate dehydrogenase. While some enzymes, such as succinyl-CoA synthetase and ATP-citrate lyase, show higher expression (Table S3b).

Under C6-HSL treatment, *Scenedesmus* shows fewer changes in TCA cycle gene expression compared to *Chlorella* and *Chlamydomonas*, likely explaining their less-affected growth. Key enzymes such as succinate dehydrogenase, isocitrate dehydrogenase, and aconitase have lower expression, indicating suppressed TCA flux. However, the higher

expression of succinyl-CoA synthetase and ATP-citrate lyase is similar behavior as *Chlorella* (Table S3c).

The addition of C6-HSL to cultures of *Chlorella*, *Scenedesmus*, and *Chlamydomonas* also led to response in gene expression across key pathways involved in fatty acid synthesis and degradation, positioning C6-HSL as a modulator of lipid accumulation in microalgae. In the initial fatty acid synthesis pathways (EC 2.3.1.12 and EC 1.2.4.1), which include enzymes like Pyruvate dehydrogenase E1, beta subunit (initiating fatty acid chain formation), each microalgae responded differently. The elongation pathways (EC 2.3.1.85 and EC 6.4.1.2), which involve enzymes like FAS1 and FAS2, showed higher expression for *Chlorella* and *Scenedesmus* in presence of C6-HSL (Fig. 5c). These genes are encoding for enzymes that are essential for production of storage lipids (Garay et al., 2014). In the pathways EC 2.3.1.179, EC 1.1.1.100,

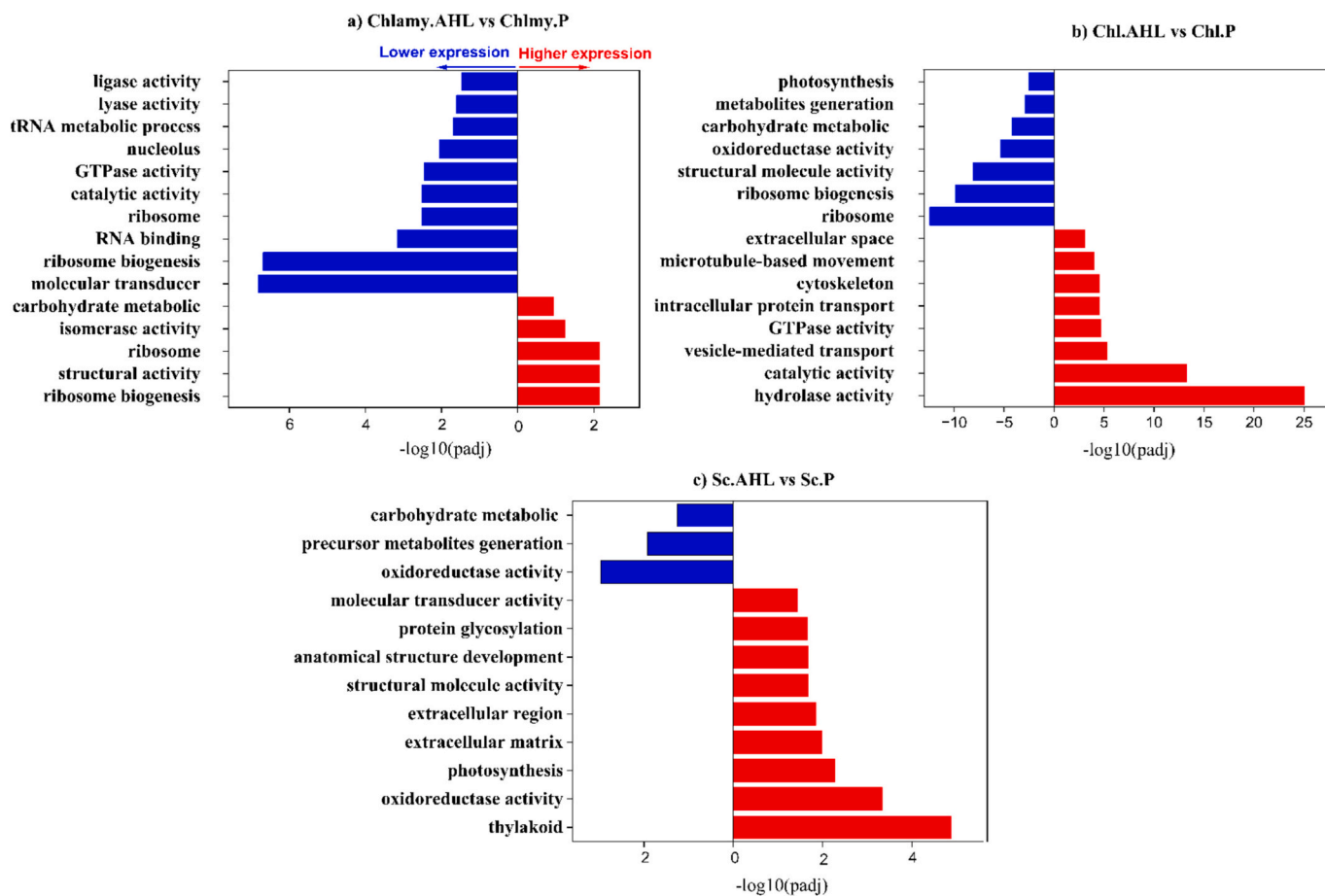


**Fig. 4.** Gene ontology enrichment bar charts of differentially expressed genes in microalgae cells a) *Chlamydomonas* (Chlmy.), b) *Chlorella* (Chl.), and c) *Scenedesmus* (Sc.) with/without C6-HSL.

and EC 1.3.1.9, gene expression varied across the microalgal species in response to C6-HSL, impacting fatty acid chain elongation, redox balance, and lipid synthesis. *Chlorella* showed the strongest response, with 17 genes which had higher expression and 9 with lower expression. *Scenedesmus* showed more moderate response of 4 genes that had higher expression and 3 with lower expression. *Chlamydomonas* exhibited a similar pattern to *Scenedesmus*, with 5 genes with higher expression and 3 with lower expression. For fatty acid degradation, *Chlamydomonas* exhibited suppression (26 down, 3 up), favoring lipid storage. The heatmap (Fig. S3) shows species-specific changes in fatty acid degradation genes under C6-HSL treatment. Under C6-HSL treatment, *Chlamydomonas* appears to shift its gene expression from lipid to carbohydrate pathways, as evidenced by the lower expression of fatty acid degradation, fatty acid elongation, and TCA cycle genes. *Scenedesmus* showed moderately lower expression, and *Chlorella* had a balanced response, indicating selective degradation that may fuel lipid production (Supporting Information Fig. S3: differential gene expression in fatty acids degradation pathway).

### 3.6. Gene expression changes in DNA replication pathways

The analysis of DNA replication-related genes under C6-HSL treatment compared with untreated microalgae samples reveals that *Scenedesmus* was minimally affected, with negligible changes in gene expression compared to *Chlorella* and *Chlamydomonas* (Fig. 6). In contrast, *Chlamydomonas* and *Chlorella* exhibited mixed patterns of higher/lower expression.

For *Chlamydomonas*, genes encoding the MCM 2–7 helicase complex showed higher expression, reflecting enhanced replication initiation,

while DNA polymerase showed slightly higher expression. Conversely, genes such as RPA and RNaseH showed slightly lower expression. In *Chlorella*, DNA polymerase and RPA showed more highly expressed genes than lowly expressed. However, similar to *Chlamydomonas*, MCM 2–7 had higher expression.

## 4. Discussion

### 4.1. Microbial signaling-mediated effects on microalgal growth and aggregation

The observed effects of C6-HSL and AS-AHLs on the growth and attachment of *Chlamydomonas*, *Chlorella*, and *Scenedesmus* can be attributed to QSSs acting as cross-kingdom signaling cues that steer cellular metabolism, with C6-HSL revealing the core transcriptomic response and AS-AHLs confirming that similar phenotypes arise under complex, sludge-derived signal mixtures. These responses change across species, reflecting their natural differences in metabolic flexibility and responsiveness to these microbial signals. AHLs are known to interact with specific regulatory proteins, leading to changes in transcriptional networks that modulate growth and metabolism (Xu et al., 2021). In contrast, the negligible effect of C6-HSL and AS-AHLs on *Scenedesmus* growth highlights its greater metabolic resistance and ability to tolerate QSSs. This may come from its robust metabolic network, which maintains core cellular processes despite external signals. Previous studies have shown that certain microalgae, including *Scenedesmus*, possess adaptable metabolic pathways that allow them to mitigate stress by reallocating resources (Calhoun et al., 2021; Singh et al., 2024). Moreover, earlier research has suggested the presence of specific metabolites

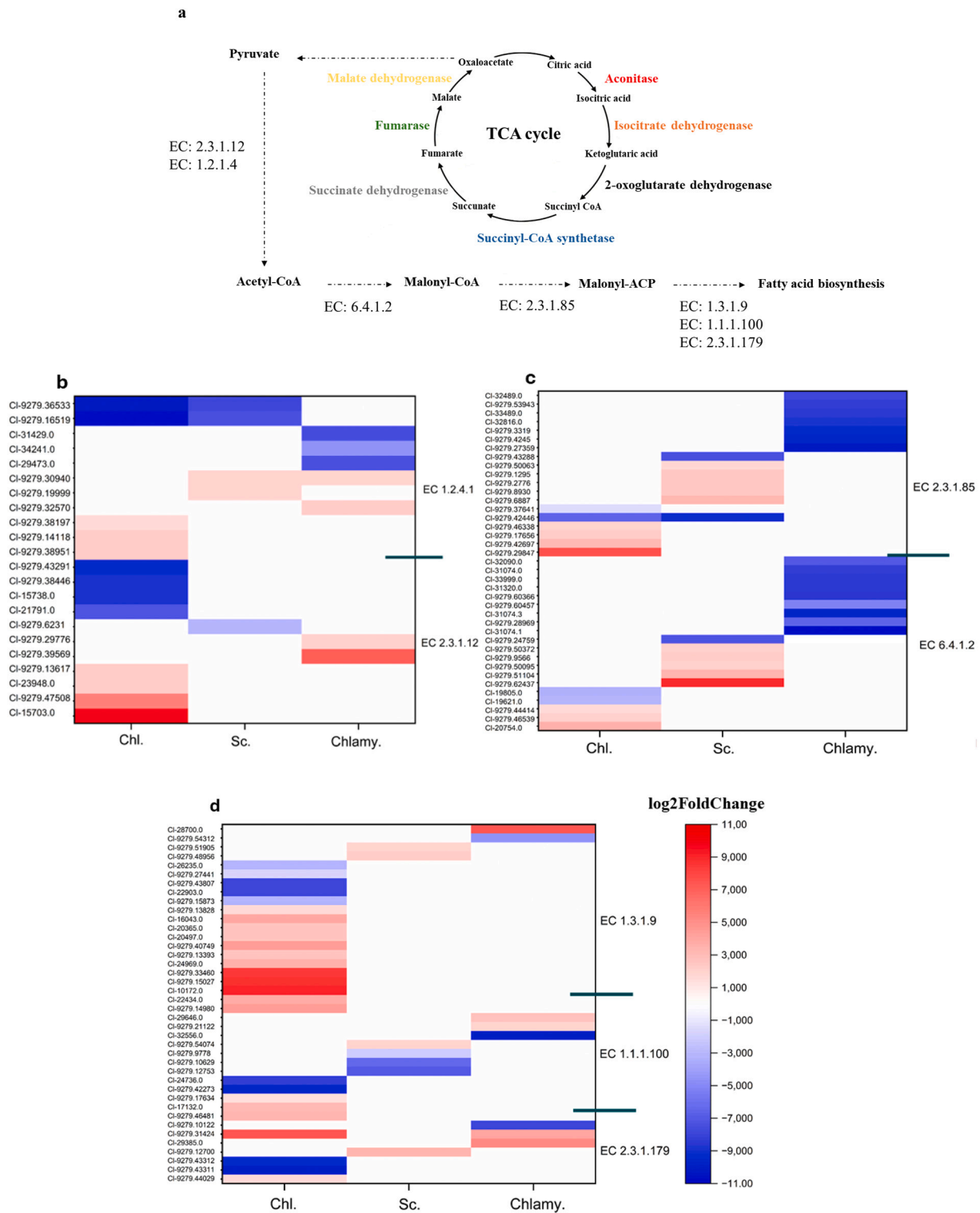


**Fig. 5.** a) TCA cycle schematic and fatty acid biosynthesis pathway that showing key enzymes affected by C6-HSL treatment. b-d) Heatmaps of differential gene expression ( $\log_2$ FoldChange) in *Chlorella* (Chl.), *Scenedesmus* (Sc.), and *Chlamydomonas* (Chlamy.).

in microalgae that could influence QSSs (Awdhesh Kumar Mishra and Kodiveri Muthukaliannan, 2022). Consequently, *Chlamydomonas* and *Chlorella* might produce distinct metabolites compared to *Scenedesmus*, potentially leading to a more noticeable impact on their growth in response to QSSs. Moreover, increased microbial attachment across all species under AHL treatments suggests that QSSs stimulate aggregation formation. AHLs are known to regulate the production of extracellular

substances in different microorganisms, which facilitate cell-surface adhesion and biofilm stability (Ou et al., 2023). Additionally, previous studies identified candidate genes in *Chlamydomonas*, *Tetradlesmus*, and *Scenedesmus* suggest that aggregation may be driven by predator sensing, cell-cell signaling, and/or structural modifications of the cell surface (Muir et al., 2024). This aggregation likely serves as a protective strategy, allowing microalgae to form structured communities that

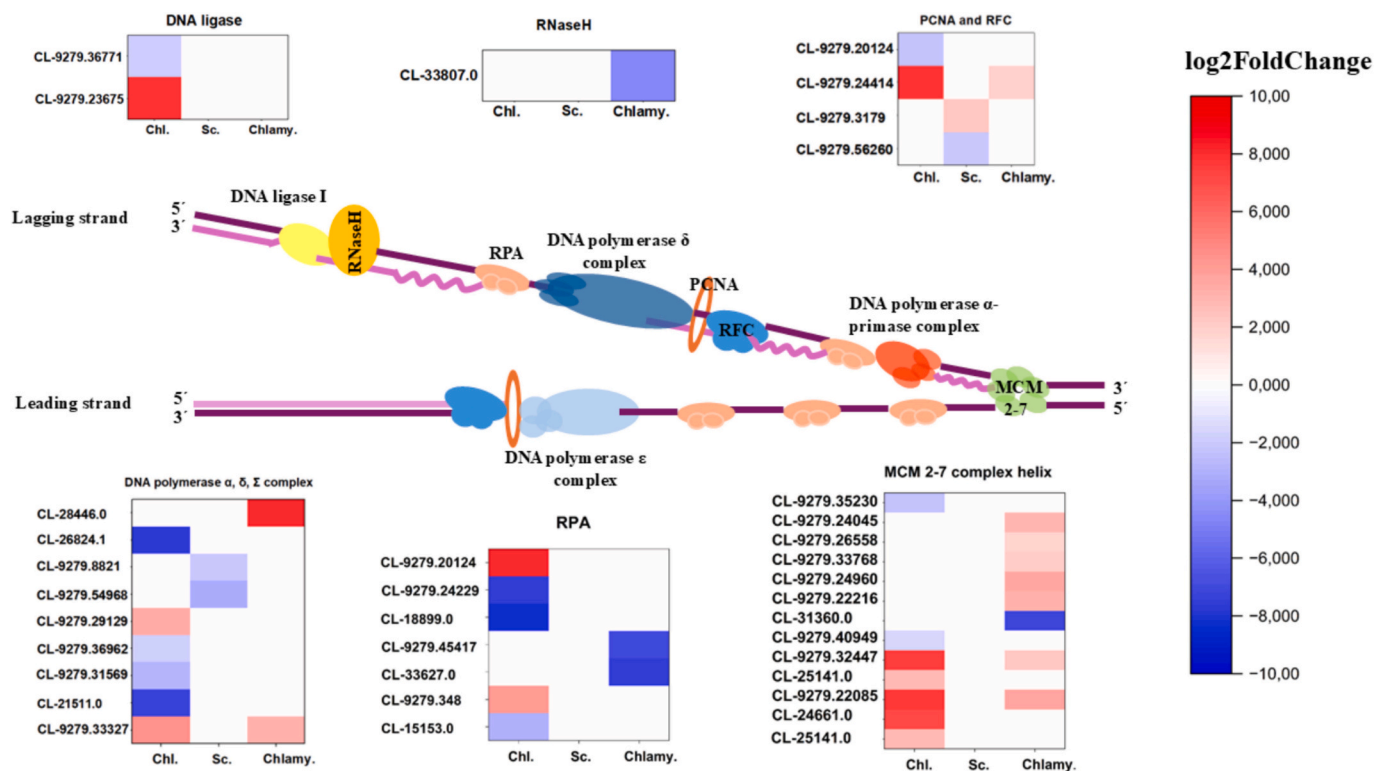


Fig. 6. Gene expression changes in DNA replication pathways under C6-HSL treatment for *Chlamydomonas* (Chlamy.), *Chlorella* (Chl.), and *Scenedesmus* (Sc.).

enhance survival under these conditions. Additionally, such enhanced aggregation can significantly improve biomass harvesting efficiency by facilitating easier and more cost-effective separation (McGrath et al., 2024).

Comparing pure C6-HSL with AS-AHL treatment shows that the overall trends were broadly consistent across strains—particularly in growth patterns, aggregation, and polysaccharide storage responses. Notably, AS-AHLs often produced stronger effects than pure C6-HSL, suggesting that the sludge extract acts as more than a single-molecule cue. This likely reflects the presence of additional AHLs in the extract, which—together with C6-HSL as the most abundant component—could collectively amplify or prolong the response relative to C6-HSL alone. With appropriate optimization, mixed AHLs recovered from activated sludge could therefore be used for the same purpose as pure signals to steer microalgal growth, aggregation, and metabolite accumulation. From an ecological perspective, AHL–microalgae interactions can be viewed as part of a broader cross-kingdom chemical dialogue. By releasing QSSs that alter algal metabolism, bacteria may indirectly shape the availability and quality of algal-derived organic carbon, oxygen, and extracellular polymeric substances, all of which influence biofilm architecture and microscale habitat structure (Dow, 2021). In return, microalgal exudates and surface properties can modulate bacterial community composition and quorum sensing dynamics, creating feedback loops that stabilize specific consortia (Mugnai et al., 2023). Thus, the AHL-induced shifts in algal lipid and polysaccharide production, as well as aggregation, may reflect ecological strategies that favor tightly coupled bacteria–algal associations.

#### 4.2. QSS-associated changes in polysaccharide and lipid

The increased polysaccharide accumulation in *Chlamydomonas* under QSSs' treatment suggests a redirection of carbon flux toward storage compounds. Polysaccharides act as energy reserves which help cells cope with environmental stress (Masi et al., 2023; Morais et al., 2022). In *Chlorella* and *Scenedesmus*, the reduction in polysaccharide

content under AHL treatments could be attributed to the reallocation of carbon resources toward lipid biosynthesis and other pathways instead of polysaccharides' accumulation. This shift likely reflects a trade-off between carbohydrate storage and the synthesis of lipids, which are essential for adaptation and membrane remodeling. Previous studies reported that in some microalgae exposed to stresses such as nitrogen deprivation, where lipid biosynthesis is prioritized over carbohydrate accumulation (Gaignard et al., 2021).

The increase in lipid accumulation under QSSs treatments, particularly in *Scenedesmus*, highlights the role of QSSs in modulating lipid metabolism. QSSs may increase expression of genes involved in fatty acid synthesis and elongation, driving the production of long-chain fatty acids for storage lipids. This behavior aligns with the known function of lipids as energy-dense molecules that provide long-term energy reserves and structural components for membranes (Van Meer et al., 2008). The shift toward increased MUFAs instead of PUFAs in response to QSSs could be due to three main reasons: 1) MUFAs are more resistant to oxidative damage than PUFAs, providing protection against oxidative stress; 2) MUFAs help maintain or adjust membrane fluidity, crucial for the cell's integrity under varying QSSs conditions; and 3) This change may reflect an adaptation in metabolic pathways influenced by quorum sensing, optimizing energy use or storage in response to environmental signals (Hulbert et al., 2006).

The differential regulation of lipid metabolism under C6-HSL exposure reflects AHL-mediated cross-kingdom metabolic steering, with species-specific strategies shaped by distinct energy demands and evolutionary adaptations. In *Chlorella*, the strong activation of fatty acid biosynthesis genes suggests metabolic reprogramming toward lipid accumulation. Higher expression of elongation enzymes like *FAS1* and *FAS2* indicates enhanced synthesis of long-chain fatty acids, possibly to build energy-dense storage lipids or to reinforce membrane structures. This mirrors *Chlorella*'s known behavior of increasing lipid storage under oxidative and nitrogen stress (Zhang et al., 2019). Additionally, moderate suppression of degradation-related genes suggests that *Chlorella* may selectively limit fatty acid breakdown to retain lipids while

maintaining flexibility in energy use. This balanced regulation could help maintain redox homeostasis which is a critical need during metabolic shifts involving NAD(P)H-linked reactions (Zhang et al., 2020). In *Scenedesmus*, the more controlled transcriptional activation implies a cautious lipid synthesis strategy. The relatively fewer genes with higher expression, alongside moderate suppression of degradation, suggests a mild shift toward lipid storage without triggering strong oxidative or energetic stress. This “balanced” lipid accumulation could be a resource-optimization approach evolved under environmental stress conditions in presence of external signals. The prior studies show that *Scenedesmus* shifts carbon toward fatty acids under phosphorus limitation, reducing carbohydrate levels to fuel lipid production (Yang et al., 2018). A similar trade-off may occur here, with C6-HSL acting as a cue to shift metabolism gently, preserving cellular stability. In *Chlamydomonas*, the transcriptomic profile indicates a distinct preference for carbohydrate over lipid storage. Although some fatty acid synthesis genes are activated, the strong suppression of degradation and moderate expression of elongation genes suggest lipid turnover is minimized. Instead, the redirection away from lipid-related pathways — including parallel lower expression in the TCA cycle — implies prioritization of carbohydrate synthesis and storage, possibly due to the lower energetic cost and compatibility with stress survival. This aligns with observed higher carbohydrate content in *Chlamydomonas*, suggesting that its defense strategy under QSSs signals favors polysaccharide accumulation over lipid biosynthesis. At the same time, QSS exposure also leads to an increase in lipid content compared with untreated controls. This dual-storage phenotype contrasts with the predominantly lipid-centric response typically observed under other stress conditions such as nitrogen starvation, indicating that QSSs induce a distinct metabolic configuration rather than simply mimicking nutrient stress and positioning QSSs not as just another stress, but as a unique tool for tailoring metabolite profiles.

#### 4.3. Transcriptomic responses to QSSs

The transcriptional responses to C6-HSL reveal that microalgae sense this bacterial QSSs as a cross-kingdom signal, triggering species-specific adaptation strategies. In *Chlamydomonas*, higher expression of carbohydrate metabolism genes suggests a redirection of carbon flux toward polysaccharide biosynthesis, likely supporting structural reinforcement and osmotic balance. Colina et al. reported that this reallocation of carbon flux supports structural reinforcement and osmotic balance, essential for survival under environmental stress conditions (Colina et al., 2020). Increased expression of polysaccharide deacetylase further indicates active cell wall remodeling, consistent with known stress responses. Although many ribosome biogenesis genes in *Chlamydomonas* showed higher expression, the observed lower expression of rRNA methylation-related genes such as fibrillar and rRNA methyltransferases suggests selective translational reprogramming. This shift likely reduces energy demands while maintaining capacity for synthesizing stress-responsive proteins. Prior findings of lower CrBUD23 (encodes rRNA methyltransferases) expression under low light in *Chlamydomonas* support this energy-conserving strategy (Liu et al., 2023). In parallel, higher expression of HSP70 chaperones and cysteine desulfurase reflects activation of protective mechanisms in both cytosol and mitochondria as mentioned in previous studies (Braymer and Lill, 2017; Maikova et al., 2016), while increased antioxidant gene expression enhances cellular defense against oxidative stress (Song et al., 2024). This suggests that AHLs trigger stress signaling that stimulates protein-folding and redox-protective pathways, helping cells mitigate damage from reactive oxygen species and maintain metabolic stability under QSSs-induced stress. Taking together, these patterns suggest that QSSs inputs are funneled through core algal stress and redox signaling pathways, which then coordinate downstream transcriptional programs. In other words, the bacterial QSSs appears to act as an upstream cue that is translated into algal responses via existing ROS-, chaperone-, and cell-

wall-associated signaling modules.

In *Chlorella*, adaptation to AHL-mediated cross-kingdom signals appears to rely more on resource-conserving strategies, favoring energy-saving and storage-oriented metabolic states. Genes related to vesicle transport and cytoskeletal organization showed higher expression, which may support intracellular trafficking and membrane remodeling (Bykov et al., 2017). Reduced expression of glycolytic enzymes indicates a decrease in energy-generating pathways, favoring survival over growth (Chung and Ng, 2024). *Scenedesmus* also exhibited lower expression of key carbohydrate metabolism genes, similar to *Chlorella*. However, this species showed higher expression of transporter and transmembrane channel genes, suggesting an emphasis on nutrient uptake or detoxification (Le Moigne et al., 2022; Shao et al., 2019). The mixed expression patterns in oxidoreductase and photosynthesis-related genes indicate a dynamic balance between conserving energy and maintaining redox and energy homeostasis. Importantly, the results of GO show that not all microalgae respond to C6-HSL by accumulating specific high-value compounds such as polysaccharides. While *Chlorella* and *Scenedesmus* primarily shift toward stress tolerance through energy conservation and membrane adaptation, *Chlamydomonas* uniquely redirects metabolic activity toward polysaccharide production. This highlights *Chlamydomonas* as a promising candidate for enhancing polysaccharide accumulation through AHL-based stimulation, offering potential for biotechnological applications where microbial signaling compounds are used to steer algal metabolite profiles. Overall, these transcriptomic patterns show that QSSs act as a molecular language that reprograms algal metabolism, highlighting a new way to tune algal traits through cross-kingdom signaling.

#### 4.4. Changes in central carbon metabolism under QSSs exposure

The lower expression of key TCA cycle genes in *Chlamydomonas*, suggests a cellular strategy to reduce mitochondrial respiration and limit ROS generation in presence of C6-HSL. Interestingly, suppression of key TCA cycle genes in *Chlamydomonas* under C6-HSL may serve as a similar protective role as described for AOX1/2 (oxidase enzymes) during photo-oxidative stress, by reducing mitochondrial electron flow and limiting ROS formation. While AOX enables dissipation of excess reducing equivalents, limiting TCA flux may prevent their accumulation upstream, offering a complementary redox control mechanism under different stress contexts (Kaye et al., 2019). C6-HSL, perceived as a microbial signal, likely triggers metabolic conservation, minimizing oxidative phosphorylation, which is energetically costly and can elevate oxidative damage in stressed cells as mentioned previously (Phillips et al., 2009). The mixed expression of malate dehydrogenase may help maintain oxaloacetate and NADH pools, supporting redox homeostasis and continuity in biosynthetic pathways (Broeks et al., 2023). In *Chlorella*, lower expression of central TCA enzymes aligns with a similar stress response; however, higher expression of ATP-citrate lyase and succinyl-CoA synthetase points to a metabolic rerouting of citrate toward acetyl-CoA production. This shift likely supports fatty acid biosynthesis — a known protective and storage mechanism during stress — and enables ATP generation via substrate-level phosphorylation when the full TCA cycle is suppressed (Phillips et al., 2009). *Scenedesmus* shows fewer changes overall, suggesting greater metabolic stability under C6-HSL. The observed lower expression of some TCA genes may reflect mild suppression of respiration, while higher ATP-citrate lyase expression again indicates a redirection of citrate to lipid biosynthesis (Fakas et al., 2025). This partial response may explain why *Scenedesmus* growth was less affected — its flexible metabolism may buffer against the energetic and oxidative stress imposed by QSSs. These expression patterns reflect conserved but distinct metabolic strategies: energy conservation in *Chlamydomonas*, metabolic rerouting in *Chlorella*, and flexibility in *Scenedesmus*.

#### 4.5. Modulation of DNA replication and cell-cycle-related genes by QSSs

In *Chlamydomonas* and *Chlorella*, the consistent higher expression of MCM2–7 helicase complex genes suggests that both species attempt to preserve or enhance replication initiation. The MCM complex is essential for unwinding DNA at replication origins, and its activation often marks the commitment to DNA synthesis (Aklilu and Culligan, 2016). Elevated expression of these genes in presence of C6-HSL may serve as a protective mechanism to ensure that critical genomic regions — perhaps those related to stress tolerance or basic cellular functions — are duplicated despite overall metabolic suppression. However, this apparent readiness for replication initiation is not fully mirrored in elongation and repair processes. The lower expression of *RPA* and *RNaseH* — both crucial for replication fork progression and RNA-DNA hybrid resolution — suggests a downregulation of elongation and post-replication repair. This decoupling between initiation and elongation could indicate a checkpoint-like regulation, where cells prepare for replication but hold back on executing full-scale synthesis until conditions improve. Such checkpoint behavior has been observed in eukaryotes under oxidative or DNA-damaging stress to prevent replication fork collapse and maintain genome integrity (Cerritelli and Crouch, 2009). In particular, *RNaseH* suppression could reflect a reduction in RNA primer removal and R-loop resolution — potentially stalling elongation to avoid replication stress-induced DNA breaks (Zhang et al., 2018). Similarly, partial suppression of *RPA* may indicate slowed DNA strand stabilization, a known strategy for reducing replication fork speed and avoiding mutagenesis. In contrast, *Scenedesmus* exhibited minimal changes in replication gene expression, which may point to a more stable cell cycle or a higher stress tolerance threshold.

#### 5. Conclusion

This study demonstrates that bacterial quorum sensing signals (QSSs), particularly C6-HSL, can act as cross-kingdom regulators of microalgal metabolism and modulate lipid and carbohydrate biosynthesis in a species-specific manner. Transcriptomic and phenotypic analyses showed that all three microalgae responded to C6-HSL with enhanced lipid accumulation, while only *Chlamydomonas* showed increased carbohydrate production. This study suggests that *Chlamydomonas* is a promising candidate for QSS-driven polysaccharide production, while *Scenedesmus*, with its robust metabolic stability and strong lipid response, emerges as a suitable target for QSS-enhanced lipid production. *Chlorella vulgaris* exhibited the broadest transcriptional response, including increased lipid biosynthesis together with suppression of photosynthesis and general metabolism. These findings support the use of QSSs to direct microalgal metabolism toward desired bioproducts and suggest their potential in species-specific bioprocessing. They also indicate that wastewater may serve not only as a nutrient source but also as a reservoir of signaling molecules. However, challenges remain, including variation in AHL composition in different wastewater streams, possible effects on microbial communities, and the trade-off between metabolite accumulation and biomass productivity, which should be addressed in future studies.

#### CRedit authorship contribution statement

**Shahla Radmehr:** Writing – original draft, Visualization, Methodology, Investigation, Conceptualization. **Johanna M. Rinta-Kanto:** Writing – review & editing. **Ville Santala:** Writing – review & editing, Supervision. **Mika Mänttari:** Writing – review & editing, Supervision.

#### Declaration of competing interest

The authors declare that they have no known competing financial interests or personal relationships that could have appeared to influence the work reported in this paper.

#### Data availability

Data will be made available on request.

#### Acknowledgements

This work was supported by Fortum and Neste Foundation. The graphical abstract was created with BioRender.

#### Appendix A. Supplementary data

Supplementary data to this article can be found online at <https://doi.org/10.1016/j.biteb.2026.102778>.

#### References

- Adams, C., Godfrey, V., Wahlen, B., Seefeldt, L., Bugbee, B., 2013. Understanding precision nitrogen stress to optimize the growth and lipid content tradeoff in oleaginous green microalgae. *Bioresour. Technol.* 131, 188–194. <https://doi.org/10.1016/j.biortech.2012.12.143>.
- Aklilu, B.B., Culligan, K.M., 2016. Molecular evolution and functional diversification of replication protein A1 in plants. *Front. Plant Sci.* 7, 33. <https://doi.org/10.3389/fpls.2016.00033>.
- Awdhesh Kumar Mishra, R., Kodiveri Muthukaliannan, G., 2022. Role of microalgal metabolites in controlling quorum-sensing-regulated biofilm. *Arch. Microbiol.* 204, 163. <https://doi.org/10.1007/s00203-022-02776-2>.
- Behera, B., Unpaprom, Y., Ramaraj, R., Maniam, G.P., Govindan, N., Paramasivan, B., 2021. Integrated biomolecular and bioprocess engineering strategies for enhancing the lipid yield from microalgae. *Renew. Sustain. Energy Rev.* 148, 111270. <https://doi.org/10.1016/j.rser.2021.111270>.
- Braymer, J.J., Lill, R., 2017. Iron-sulfur cluster biogenesis and trafficking in mitochondria. *J. Biol. Chem.* 292, 12754–12763. <https://doi.org/10.1074/jbc.R117.787101>.
- Broeks, M.H., Meijer, N.W.F., Westland, D., Bosma, M., Gerrits, J., German, H.M., Ciapaite, J., van Karnebeek, C.D.M., Wanders, R.J.A., Zwartkruis, F.J.T., Verhoeven-Duif, N.M., Jans, J.J.M., 2023. The malate-aspartate shuttle is important for *de novo* serine biosynthesis. *Cell Rep.* 42, 113043. <https://doi.org/10.1016/j.celrep.2023.113043>.
- Bykov, Y.S., Schaffer, M., Dodonova, S.O., Albert, S., Plitzko, J.M., Baumeister, W., Engel, B.D., Briggs, J.A., 2017. The structure of the COPI coat determined within the cell. *eLife* 6, e32493. <https://doi.org/10.7554/eLife.32493>.
- Caetano, P.A., do Nascimento, T.C., Fernandes, A.S., Nass, P.P., Vieira, K.R., Maróstica Junior, M.R., Jacob-Lopes, E., Zepka, L.Q., 2022. Microalgae-based polysaccharides: insights on production, applications, analysis, and future challenges. *Biocatal. Agric. Biotechnol.* 45, 102491. <https://doi.org/10.1016/j.bcab.2022.102491>.
- Calhoun, S., Bell, T.A.S., Dahlin, L.R., Kunde, Y., LaButti, K., Louie, K.B., Kufin, A., Trean, D., Dilworth, D., Mihaltcheva, S., Daum, C., Bowen, B.P., Northen, T.R., Guarnieri, M.T., Starkenburg, S.R., Grigoriev, I.V., 2021. A multi-omic characterization of temperature stress in a halotolerant *Scenedesmus* strain for algal biotechnology. *Commun. Biol.* 4, 333. <https://doi.org/10.1038/s42003-021-01859-y>.
- Cerritelli, S.M., Crouch, R.J., 2009. Ribonuclease H: the enzymes in eukaryotes. *FEBS J.* 276, 1494–1505. <https://doi.org/10.1111/j.1742-4658.2009.06908.x>.
- Chung, C.-W., Ng, I.-S., 2024. Tailoring nitrogen and phosphorus levels for tunable glycogen and protein production in halophilic *Cyanobacterium apoinum* PCC10605. *Bioresour. Technol.* 406, 131052. <https://doi.org/10.1016/j.biortech.2024.131052>.
- Colina, F.J., Carbó, M., Cañal, M.J., Vallerod, L., 2020. A complex metabolic rearrangement towards the accumulation of glycerol and sugars consequence of a proteome remodeling is required for the survival of *Chlamydomonas reinhardtii* growing under osmotic stress. *Environ. Exp. Bot.* 180, 104261. <https://doi.org/10.1016/j.envexpbot.2020.104261>.
- Coolahan, M., Whalen, K.E., 2025. A review of quorum-sensing and its role in mediating interkingdom interactions in the ocean. *Commun. Biol.* 8, 179. <https://doi.org/10.1038/s42003-025-07608-9>.
- Deshmukh, S., Kumar, R., Bala, K., 2019. Microalgae biodiesel: a review on oil extraction, fatty acid composition, properties and effect on engine performance and emissions. *Fuel Process. Technol.* 191, 232–247. <https://doi.org/10.1016/j.fuproc.2019.03.013>.
- Dow, L., 2021. How do quorum-sensing signals mediate algae–bacteria interactions? *Microorganisms* 9, 1391. <https://doi.org/10.3390/microorganisms9071391>.
- DuBois, M., Gilles, K.A., Hamilton, J.K., Rebers, P.A., Smith, Fred, 1956. Colorimetric method for determination of sugars and related substances. *Anal. Chem.* 28, 350–356. <https://doi.org/10.1021/ac60111a017>.
- Fakas, S., Odunsi, A., Fakas, S., Odunsi, A., 2025. ATP citrate lyase in lipid metabolism: comparative insights across eukaryotes with emphasis on *Yarrowia lipolytica*. *Lipidology* 2 (4), 20. <https://doi.org/10.3390/lipidology2040020>.
- Ferreira, G.F., Ríos Pinto, L.F., Maciel Filho, R., Fregolente, L.V., 2019. A review on lipid production from microalgae: association between cultivation using waste streams and fatty acid profiles. *Renew. Sustain. Energy Rev.* 109, 448–466. <https://doi.org/10.1016/j.rser.2019.04.052>.

- Gaignard, C., Zissis, G., Buso, D., 2021. Influence of different abiotic factors on lipid production by microalgae – a review. *OCL* 28, 57. <https://doi.org/10.1051/ocl/2021045>.
- Garay, L.A., Boundy-Mills, K.L., German, J.B., 2014. Accumulation of high-value lipids in single-cell microorganisms: a mechanistic approach and future perspectives. *J. Agric. Food Chem.* 62, 2709–2727. <https://doi.org/10.1021/jf4042134>.
- Gouda, M., Tadda, M.A., Zhao, Y., Farmanullah, F., Chu, B., Li, X., He, Y., 2022. Microalgae bioactive carbohydrates as a novel sustainable and eco-friendly source of prebiotics: emerging health functionality and recent technologies for extraction and detection. *Front. Nutr.* 9, 806692. <https://doi.org/10.3389/fnut.2022.806692>.
- Hulbert, A.J., Faulks, S.C., Buffenstein, R., 2006. Oxidation-resistant membrane phospholipids can explain longevity differences among the longest-living rodents and similarly-sized mice. *J. Gerontol. A Biol. Sci. Med. Sci.* 61, 1009–1018. <https://doi.org/10.1093/gerona/61.10.1009>.
- Iverson, S.J., Lang, S.L.C., Cooper, M.H., 2001. Comparison of the Bligh and dyer and Folch methods for total lipid determination in a broad range of marine tissue. *Lipids* 36, 1283–1287. <https://doi.org/10.1007/s11745-001-0843-0>.
- Kaye, Y., Huang, W., Clowez, S., Saroussi, S., Idoine, A., Sanz-Luque, E., Grossman, A.R., 2019. The mitochondrial alternative oxidase from *Chlamydomonas reinhardtii* enables survival in high light. *J. Biol. Chem.* 294, 1380–1395. <https://doi.org/10.1074/jbc.RA118.004667>.
- Le Moigne, T., Sarti, E., Nourisson, A., Zaffagnini, M., Carbone, A., Lemaire, S.D., Henri, J., 2022. Crystal structure of chloroplast fructose-1,6-bisphosphate aldolase from the green alga *Chlamydomonas reinhardtii*. *J. Struct. Biol.* 214, 107873. <https://doi.org/10.1016/j.jsb.2022.107873>.
- Liu, C., Guo, H., Zhao, X., Zou, B., Sun, T., Feng, J., Zeng, Z., Wen, X., Chen, J., Hu, Z., Lou, S., Li, H., 2023. Overexpression of 18S rRNA methyltransferase CrBUD23 enhances biomass and lutein content in *Chlamydomonas reinhardtii*. *Front. Bioeng. Biotechnol.* 11, 1102098. <https://doi.org/10.3389/fbioe.2023.1102098>.
- Lyu, W., Zhang, S., Xie, Y., Chen, R., Hu, X., Wang, B., Guo, W., Wang, H., Xing, J., Zhou, D., 2022. Effects of the exogenous N-acylhomoserine lactones on the performances of microalgal-bacterial granular consortia. *Environ. Pollut. Bioavail.* 34, 407–418. <https://doi.org/10.1080/26395940.2022.2123046>.
- Maikova, A., Zalutskaya, Z., Lapina, T., Ermilova, E., 2016. The HSP70 chaperone machines of *Chlamydomonas* are induced by cold stress. *J. Plant Physiol.* 204, 85–91. <https://doi.org/10.1016/j.jplph.2016.07.012>.
- Mangope, K., Kaseke, T., Fawole, O.A., 2025. Spray-drying microencapsulation of fixed oils: an innovative and sustainable technology to enhance oxidative stability, functionality and application in food systems. *Appl. Food Res.* 5, 101200. <https://doi.org/10.1016/j.afres.2025.101200>.
- Masi, A., Leonelli, F., Scognamiglio, V., Gasperuzzo, G., Antonacci, A., Terzidis, M.A., 2023. *Chlamydomonas reinhardtii*: a factory of nutraceutical and food supplements for human health. *Molecules* 28, 1185. <https://doi.org/10.3390/molecules28031185>.
- McGrath, S.J., Laamanen, C.A., Senhorinho, G.N.A., Scott, J.A., 2024. Microalgal harvesting for biofuels – options and associated operational costs. *Algal Res.* 77, 103343. <https://doi.org/10.1016/j.algal.2023.103343>.
- Mohamed, A., Owis, E., Abdel-Fattah, G., Eltanahy, E., 2025. Optimising *Chlorella vulgaris* bioflocculation by Aspergillus Niger pellets and their application in wastewater treatment and lipid production. *Microb. Cell Fact.* 24, 229. <https://doi.org/10.1186/s12934-025-02849-z>.
- Morais, M.G., Santos, T.D., Moraes, L., Vaz, B.S., Morais, E.G., Costa, J.A.V., 2022. Exopolysaccharides from microalgae: production in a biorefinery framework and potential applications. *Bioresour. Technol. Rep.* 18, 101006. <https://doi.org/10.1016/j.biteb.2022.101006>.
- Mugnai, S., Derossi, N., Hendlin, Y., 2023. Algae communication, conspecific and interspecific: the concepts of phycosphere and algal-bacteria consortia in a photobioreactor (PBR). *Plant Signal. Behav.* 18, e2148371. <https://doi.org/10.1080/15592324.2022.2148371>.
- Muir, E., Grossman, A.R., Chisti, Y., Fedrizzi, B., Guieysse, B., Plouviez, M., 2024. Self-aggregation for sustainable harvesting of microalgae. *Algal Res.* 83, 103685. <https://doi.org/10.1016/j.algal.2024.103685>.
- Mukherjee, S., Bassler, B.L., 2019. Bacterial quorum sensing in complex and dynamically changing environments. *Nat. Rev. Microbiol.* 17, 371–382. <https://doi.org/10.1038/s41579-019-0186-5>.
- Ou, Z., Chen, X., Wu, X., Zhou, C., Zhang, K., Luo, J., Fang, F., Sun, Y., Li, M., Feng, Q., 2023. N-acyl homoserine lactone mediating initial adhesion of microalgal biofilm formation. *Environ. Res.* 233, 116446. <https://doi.org/10.1016/j.envres.2023.116446>.
- Pereira-Santana, A., Gamboa-Tuz, S.D., Zhao, T., Schranz, M.E., Vinuesa, P., Bayona, A., Rodríguez-Zapata, L.C., Castano, E., 2020. Fibrillar evolution through the Tree of Life: comparative genomics and microsynteny network analyses provide new insights into the evolutionary history of Fibrillar. *PLoS Comput. Biol.* 16, e1008318. <https://doi.org/10.1371/journal.pcbi.1008318>.
- Phillips, D., Aponte, A.M., French, S.A., Chess, D.J., Balaban, R.S., 2009. Succinyl-CoA synthetase is a phosphate target for the activation of mitochondrial metabolism. *Biochemistry* 48, 7140–7149. <https://doi.org/10.1021/bi900725c>.
- Rajpoot, A.S., Choudhary, T., Chelladurai, H., Nath Verma, T., Shende, V., 2022. A comprehensive review on bioplastic production from microalgae. *Mater. Today Proc.* 56, 171–178. <https://doi.org/10.1016/j.matpr.2022.01.060>.
- Scranton, M.A., Ostrand, J.T., Fields, F.J., Mayfield, S.P., 2015. *Chlamydomonas* as a model for biofuels and bio-products production. *Plant J.* 82, 523–531. <https://doi.org/10.1111/tpj.12780>.
- Shao, Z., Zhang, P., Lu, C., Li, S., Chen, Z., Wang, X., Duan, D., 2019. Transcriptome sequencing of *Saccharina japonica* sporophytes during whole developmental periods reveals regulatory networks underlying alginate and mannitol biosynthesis. *BMC Genomics* 20, 975. <https://doi.org/10.1186/s12864-019-6366-x>.
- Singh, R.P., Yadav, P., Sharma, H., Kumar, A., Hashem, A., Abd Allah, E.F., Gupta, R.K., 2024. Unlocking the adaptation mechanisms of the oleaginous microalga *Scenedesmus* sp. BHU1 under elevated salt stress: a physicochemical, lipidomics and transcriptomics approach. *Front. Microbiol.* 15, 1475410. <https://doi.org/10.3389/fmicb.2024.1475410>.
- Song, X., Kong, F., Liu, B.-F., Song, Q., Ren, N.-Q., Ren, H.-Y., 2024. Antioxidants alleviated low-temperature stress in microalgae by modulating reactive oxygen species to improve lipid production and antioxidant defense. *Bioresour. Technol.* 413, 131451. <https://doi.org/10.1016/j.biortech.2024.131451>.
- Sreelakshmi, M., Arunkumar, K., 2025. Microalgal neutral lipid accumulation: cellular mechanism and ways to improve biodiesel production. *Bioenergy Res.* 18, 50. <https://doi.org/10.1007/s12155-025-10851-x>.
- Sun, W., Zhang, T., Zhong, A., Yang, G., Yang, Songqi, Luo, X., Yang, Shenghui, Liu, H., Luo, G., 2025. Effects of light on municipal wastewater treatment efficiency, byproduct generation, and growth of *Scenedesmus quadricauda*. *J. Water Process Eng.* 109117. <https://doi.org/10.1016/j.jwpe.2025.109117>.
- Udayan, A., Pandey, A.K., Sharma, P., Sreekumar, N., Kumar, S., 2021. Emerging industrial applications of microalgae: challenges and future perspectives. *Syst. Microbiol. Biomanuf.* 1, 411–431. <https://doi.org/10.1007/s43393-021-00038-8>.
- Udayan, A., Pandey, A.K., Sirohi, R., Sreekumar, N., Sang, B.-I., Sim, S.-J., Kim, S.H., Pandey, A., 2023. Production of microalgae with high lipid content and their potential as sources of nutraceuticals. *Phytochem. Rev.* 22, 833–860. <https://doi.org/10.1007/s11101-021-09784-y>.
- Van Meer, G., Voelker, D.R., Feigenson, G.W., 2008. Membrane lipids: where they are and how they behave. *Nat. Rev. Mol. Cell Biol.* 9, 112–124. <https://doi.org/10.1038/nrm2330>.
- Wang, J., Ding, L., Li, K., Schmieder, W., Geng, J., Xu, K., Zhang, Y., Ren, H., 2017. Development of an extraction method and LC–MS analysis for N-acylated-l-homoserine lactones (AHLs) in wastewater treatment biofilms. *J. Chromatogr. B* 1041–1042, 37–44. <https://doi.org/10.1016/j.jchromb.2016.11.029>.
- Wang, H., Wu, P., Zheng, D., Deng, L., Wang, W., 2022. N-Acyl-Homoserine Lactone (AHL)-mediated microalgal-bacterial communication driving *Chlorella*-activated sludge bacterial biofloc formation. *Environ. Sci. Technol.* 56, 12645–12655. <https://doi.org/10.1021/acs.est.2c00905>.
- Wu, J., Gu, X., Yang, D., Xu, S., Wang, S., Chen, X., Wang, Z., 2021. Bioactive substances and potentiality of marine microalgae. *Food Sci. Nutr.* 9, 5279–5292. <https://doi.org/10.1002/fsn3.2471>.
- Wu, X., Kong, L., Pan, J., Feng, Y., Liu, S., 2022. Metagenomic approaches to explore the quorum sensing-mediated interactions between algae and bacteria in sequence membrane photo-bioreactors. *Front. Bioeng. Biotechnol.* 10, 851376. <https://doi.org/10.3389/fbioe.2022.851376>.
- Xu, Y., Curtis, T., Dolfin, J., Wu, Y., Rittmann, B.E., 2021. N-acyl-homoserine-lactones signaling as a critical control point for phosphorus entrapment by multi-species microbial aggregates. *Water Res.* 204, 117627. <https://doi.org/10.1016/j.watres.2021.117627>.
- Yang, F., Xiang, W., Li, T., Long, L., 2018. Transcriptome analysis for phosphorus starvation-induced lipid accumulation in *Scenedesmus* sp. *Sci. Rep.* 8, 16420. <https://doi.org/10.1038/s41598-018-34650-x>.
- Zhang, C., Li, Q., Fu, L., Zhou, D., Crittenden, J.C., 2018. Quorum sensing molecules in activated sludge could trigger microalgae lipid synthesis. *Bioresour. Technol.* 263, 576–582. <https://doi.org/10.1016/j.biortech.2018.05.045>.
- Zhang, L., Wang, N., Yang, M., Ding, K., Wang, Y.-Z., Huo, D., Hou, C., 2019. Lipid accumulation and biodiesel quality of *Chlorella pyrenoidosa* under oxidative stress induced by nutrient regimes. *Renew. Energy* 143, 1782–1790. <https://doi.org/10.1016/j.renene.2019.05.081>.
- Zhang, W., Gao, J., Zhou, W., 2020. Transcriptome-based analysis of euglena gracilis lipid metabolic pathways under light stress. *Turk. J. Fish. Aquat. Sci.* 20 (6), 453–465. [https://doi.org/10.4194/1303-2712-v20\\_6\\_04](https://doi.org/10.4194/1303-2712-v20_6_04).